Electronic Supplementary Material (ESI) for Nanoscale.

Contents

S1: Experimental Details

Chemical Reagents

Citrate-capped silver nanoparticles (NPs) of *ca.* "50 nm diameter" (Nanoxact, 0.02 mg mL^{-1} silver, 2 mM sodium citrate) were purchased from NanoComposix, USA. Representative TEM images of these NPs are presented in section S7.

Tomographic Reconstruction

The dual-axis tilt-series of two silver nanoparticle agglomerates (citrate capped, nominally 50 nm diameter) were acquired using a FEI Talos 200c FEG-TEM at a 73000 × magnification, with a pixel size of 1.431 Å per pixel. The dual-axis series consists of two perpendicular tilt-series that are combined for reconstruction. The tilt-series were reconstructed using IMOD 4.9 to give tomograms as a series of *z*-stacked images (477 and 410 images for the two agglomerates).

Segmentation of the particles was carried out using ImageJ software, involving contrast enhancement followed by application of a Gaussian Blur (standard deviation, σ = 2 pixels), and threshold cropping (IsoData method). The resulting nanoparticle substacks were denoised using non-local-means denoising (σ = 30 pixels) and thresholded (IsoData method) to give binary *z*-stacks for 13 individual nanoparticles.

Tomographic volume determination was achieved by voxel counting using the voxel counter function in ImageJ. 3D rendering of the nanoparticles was attained using TomViz 1.3.0,[1] using the colour map bone_matlab. A Gaussian Blur (σ = 2.5 voxels) was applied to the 3D volume and images acquired down the *x*, *y* and *z* axes. 2D Z-projections were obtained by creating a flattened *z*-projection of maximum intensity from the binary images in ImageJ. The maximum Feret diameter was measured and taken as the diameter to calculate the volume of the circumscribed sphere, and the minimum Feret diameter was measured to calculate the Feret ratio.

Transmission Electron Microscopy

Transmission Electron Microscopy (TEM) imaging was carried out using a JEOL JEM-3000F instrument with an accelerating voltage of 300 kV. The samples were prepared by drop-casting the silver nanoparticle suspension (48 pM silver nanoparticles, 2 mM sodium citrate) onto carbon grids (Agar Scientific Ltd., UK) and allowing them to dry. Image extraction was performed using ImageJ software. Representative TEM images are presented in the SI section S5.

Dynamic Light Scattering

DLS measurements were carried out using a Malvern Zetasizer Nano ZS (Malvern, Herrenberg, Germany) equipped with a 633 nm He-Ne laser at an angle of 173°. Data analysis was performed

using Malvern's Zetasizer Software, version 7.12. A 1 mL suspension of 48 pM citrate-capped silver nanoparticles was filtered using a Millex ® GV Durapore 0.22 µm filter (Merck, Ireland) into a disposable polystyrene microcuvette with a path length of 10 mm. The measurements were carried out under thermostated conditions at 25°C. The intensity, volume and number size distributions, intensity, volume, number and Z-average diameter and the polydispersity index (PdI) were obtained from the autocorrelation function using the general purpose mode.

Nanoparticle Tracking Analysis

Nanoparticle Tracking Analysis (NTA) measurements were carried out at room temperature using a NanoSight LM10 (Nanosight, Amesbury, UK), in a sample chamber equipped with a 638 nm laser. A suspension of 48 pM citrate-capped silver nanoparticles was diluted 100-fold with deionised water and injected into the chamber with sterile syringes (BsD, Discardit II, New Jersey, USA). The samples were measured for 30 s at 30 fps. Data analysis was carried out using NTA 3.2 software.

S2: Example of Raw Tomogram Image

The dual-axis TEM tilt-series of two silver nanoparticle agglomerates were acquired using a FEI Talos 200c FEG-TEM at a 73000 × magnification, with a pixel size of 1.431 Å per pixel. These were aligned using IMOD to give tomograms as a series of *z*-stacked images. For the two nanoparticle agglomerates, the tomograms consisted of 477 and 410 *z*-slices respectively. Figure S2 depicts a representative raw tomogram *z*-slice (slice 198 out of 410) of one of the nanoparticle agglomerates prior to particle segmentation and reconstruction. The light features observed in the nanoparticles in contrast to the dark background are discussed in the main text and section S4.

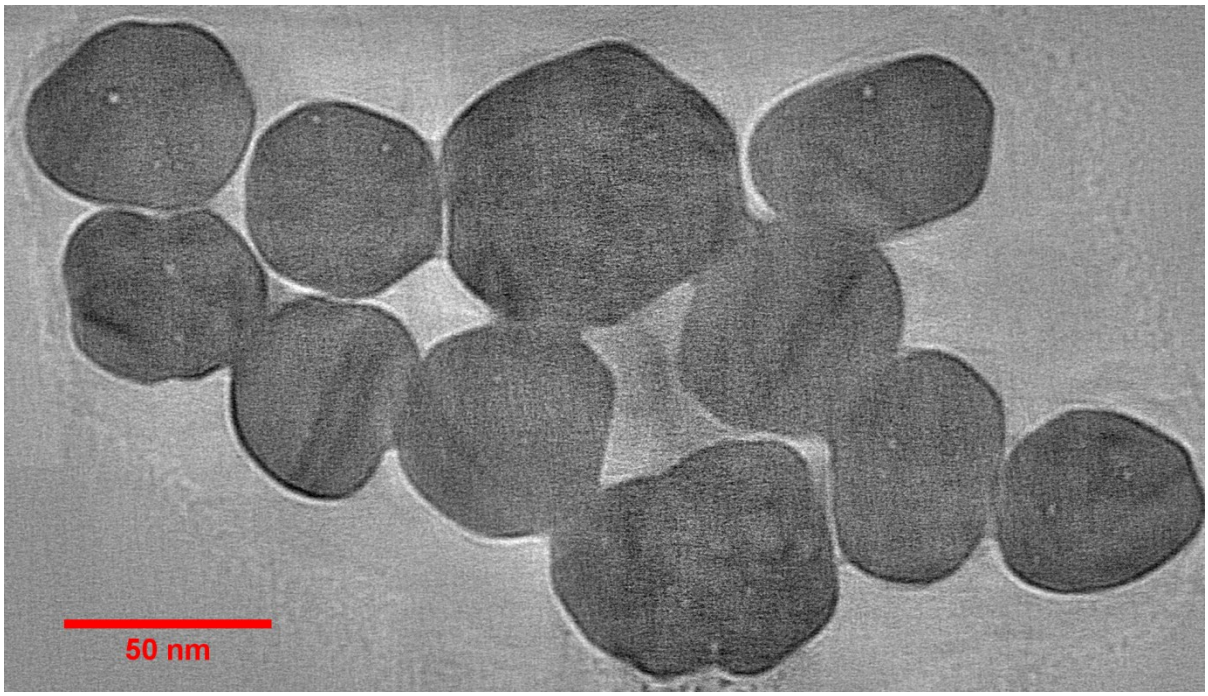

Figure S2. Raw tomogram *z*-slice image (image 198 out of 410) for a silver nanoparticle agglomerate prior to segmentation and 3D reconstruction.

S3: Details of Reconstruction Process by Electron Tomography

The flow chart in Figure S3 depicts the key stages in the 3D reconstruction of the silver nanoparticles by Electron Tomography. As described in the section S1, the dual-axis TEM tilt-series of two silver nanoparticle agglomerates (consisting of 7 and 12 nanoparticles) were acquired using a FEI Talos 200c FEG-TEM instrument under 73000 × magnification. These tilt-series were aligned and reconstructed using IMOD 4.9 to give tomograms of the two nanoparticle agglomerates as a series of *z*-stack images, consisting of 477 and 410 images, with a pixel size of 0.1431 nm per pixel, corresponding to a voxel (3D pixel) volume of 2.93×10^{-3} nm^3 per voxel. The particles were then segmented using ImageJ; this involved contrast enhancement of the entire stack followed by the application of a Gaussian Blur (standard deviation, σ = 2 pixels) and threshold cropping using the IsoData method.[2] Of the 12 particles in the second nanoparticle agglomerate, 6 were discarded as part of this process due to missing volumes at the beginning or end of the *z*-stack, leaving 13 particles as individual *z*-stacks. These stacks were then denoised using non-local-means denoising (σ = 30 pixels) and thresholded (IsoData method) to afford the *binary z*-stacks required for the subsequent volume calculation.

The nanoparticle volumes were determined by use of the Voxel Counter function in ImageJ, which counts all voxels corresponding to the nanoparticle in each *z*-slice; the volume of a voxel is known as described above from the tomogram reconstruction, hence affording a volume for each of the 13 nanoparticles. The nanoparticles were then rendered in 3D using the freely-available software Tomviz 1.3.0,[1] and false-coloured using the colour map bone_matlab. A Gaussian Blur (σ = 2.5 voxels) was applied to the 3D volume and images were acquired as viewed down the *x*, *y* and *z* axes; examples of these images are presented in the main text, Figure 1. A video of 12 of these nanoparticles rendered in 3D is available online; the video depicts each nanoparticle rotating about the designated *y* axis.

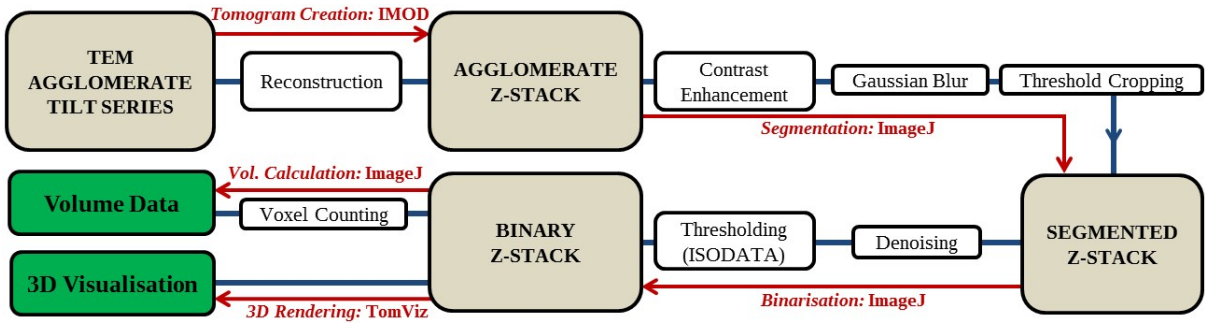

Figure S3. Flow chart depicting stages in silver nanoparticle reconstruction by Electron Tomography. The key stages and software used are depicted in red.

S4: Images of Silver Nanoparticle Voids

Figure S4a presents representative *z*-slice images of the voids present in the silver nanoparticles, as described in the main text. A video is also available online depicting these voids frame by frame through the *z*-stack of the nanoparticle at 10 fps. For one nanoparticle, 44 voids were identified with an average diameter of 2.58 ± 0.20 nm and a standard deviation of 1.30 nm. It should be noted that several smaller similar features are present in these images; however such features are at the limit of resolution for this technique. These features last for around 4 frames; this corresponds to a void diameter of 0.57 nm, or *ca.* 6 Ag atoms. However, it should be noted that voids of these size are nearly 6 orders of magnitude smaller than the total volume of the particle, and hence their disregarding here has negligible effect.

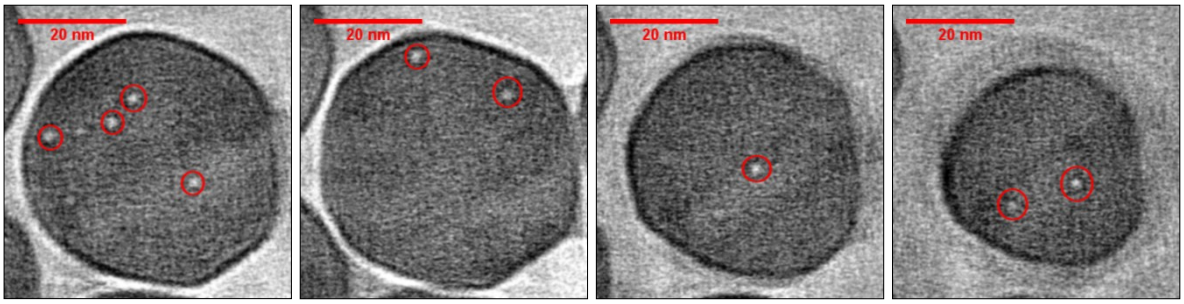

Figure S4a. Representative images depicting voids in the silver nanoparticles for four different *z*-slices. On average, each void lasts for 18 frames, corresponding to a spherical diameter of 2.58 nm.

Figure S4b presents 3D rendered images of the voids inside i) a cuboid volume of the same particle and ii) in the complete particle.

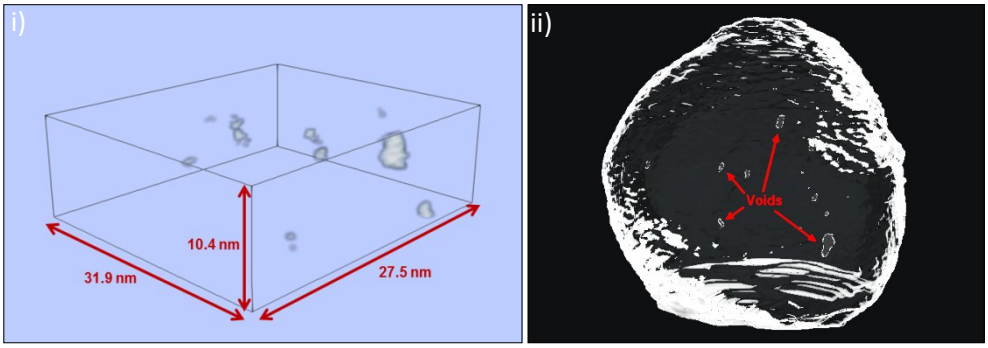

Figure S4b. i) Cubic volume segment of a silver nanoparticle depicting the voids as 3D volumes. ii) Complete nanoparticle with voids rendered in Autodesk Fusion.

S5: Comparison of Volumes Calculated from ET and 2D Projections

Figure S5 presents the cumulative frequency volume distributions as calculated directly by voxel counting the 3D reconstructed nanoparticles obtained from Electron Tomography, and by applying optimised correction factors to 2D projections of the same nanoparticles. The optimisation of these correction factors is detailed in the main text. There is an excellent agreement between the two methods; the mean volumes calculated directly from the reconstruction and from the projections are 7.61 ± 0.47 × 10^{-23} m^3 and 7.65 ± 0.49 × 10^{-23} m^3 respectively, corresponding to an overestimation of the volume by ca. 0.5% when calculating the nanoparticle volume from the 2D projections.

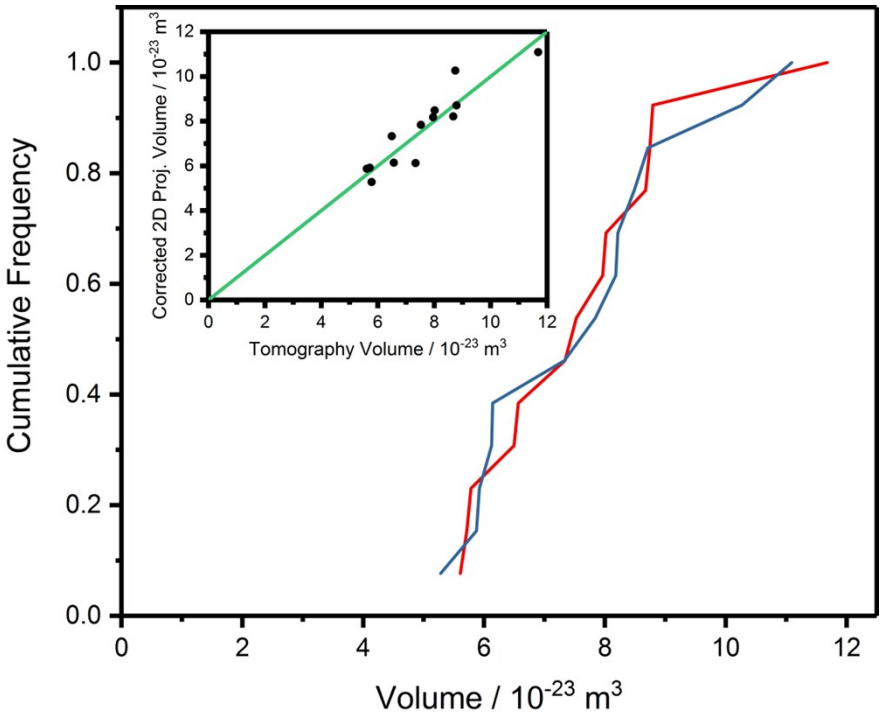

Figure S5. Cumulative frequency volume distributions as calculated from voxel counting 3D tomographic reconstructions of nanoparticles (red line) or by applying optimised correction factors determined by the Feret ratio to 2D projections of the nanoparticles, as they would be viewed in TEM imaging (blue lines). Inlay depicts the correlation between the volumes calculated by using the two methods.

S6: Volume Reconstruction by Projection Area Method

As described in the main text, the 3D volume of a nanoparticle can be estimated from the area of the 2D projection. This is achieved by calculating the radius of a circle of equivalent area to the 2D *z*-projection of the nanoparticle and then using this radius to calculate the volume of a sphere. A comparison between the cumulative frequency volume distributions obtained by this method and tomographic reconstruction is presented in Figure S6; the inlay depicts the correlation between the volumes calculated by these methods. There is an excellent agreement between the two distributions; the mean volume obtained by this method is $7.87 \pm 0.45 \times 10^{-23}$ m^3, compared to $7.61 \pm 0.47 \times 10^{-23}$ m^3 calculated from Electron Tomography, corresponding to an overestimation of the volume by 3.5%. As highlighted in the main text, whilst this is a larger overestimation compared to the method used in section S5, the method is independent of the tomography study (the method used in section S5 obtained optimised correction factors based on the results from tomography) and hence can have a general application to other populations of nanoparticles. Furthermore, this estimation can be interpreted as a measure of the minimum error to which the nanoparticle volume can be estimated, crucial in determining the error in particle number concentration calculations.

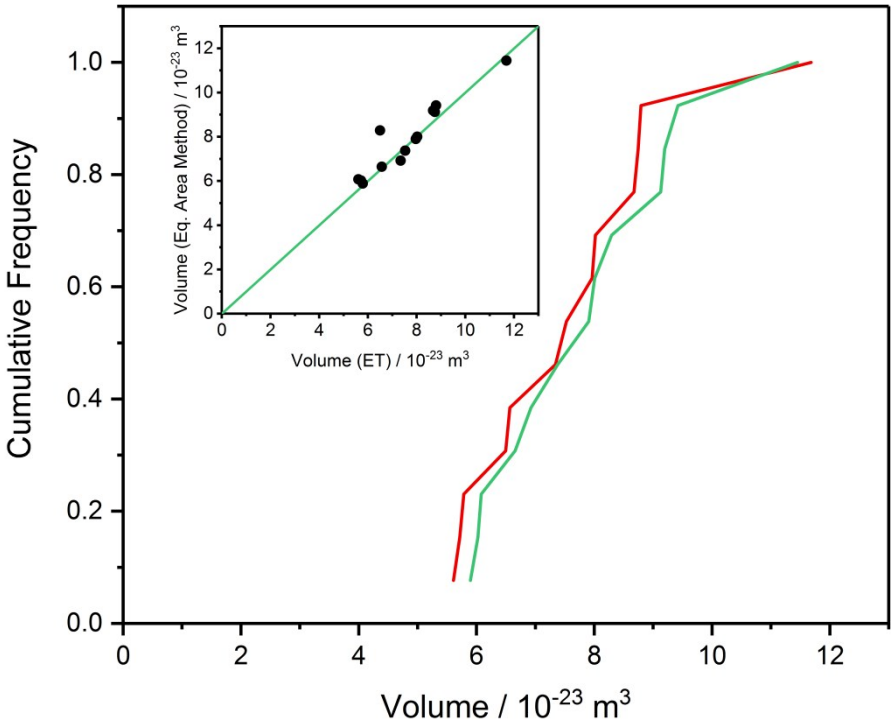

Figure S6. Cumulative frequency volume distributions as calculated from voxel counting 3D tomographic reconstructions of nanoparticles (red line) or by calculating the a spherical volume based on the radius of a circle of equivalent area to a nanoparticle as would be viewed in TEM imaging (blue lines). Inlay depicts the correlation between the volumes calculated by using the two methods.

S7: TEM Images of Silver Nanoparticles

Transmission Electron Microscopy (TEM) imaging of the silver nanoparticles was carried out using a JEOL JEM-3000F instrument at an accelerating voltage of 300 kV. The samples were prepared by drop-casting suspensions of 48 pM silver nanoparticles (2 mM sodium citrate) onto carbon grids (Agar Scientific Ltd., UK) and allowing the grids to dry. The images were subsequently extracted using ImageJ software. Figure S7 presents representative TEM images of these nanoparticles.

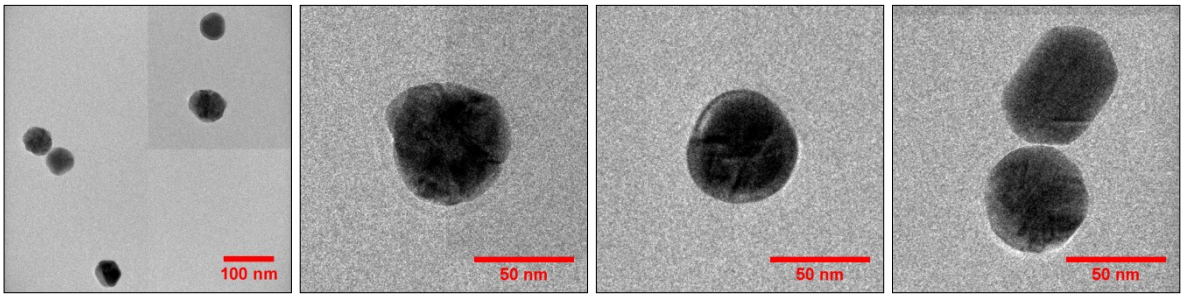

Figure S7. Representative TEM images of commercial spherical citrate-AgNPs of nominally 50 nm diameter (NanoXact, 0.02 mg mL^{-1} silver, 2 mM sodium citrate)

S8: Comparison of Distributions Obtained from DLS

Figure S8 portrays the normalised intensity, volume and number hydrodynamic radii distributions obtained from DLS measurements using the Malvern Zetasizer Nano ZS as well as the corresponding mean radii and associated standard deviation. The widely-accepted parameters to report from DLS measurements are that of the intensity distribution and the *z*-average radii.[3] Acknowledging the tendency of the intensity distribution obtained from DLS to overestimate the radius based on the inherent bias towards larger particles, as well as the difficulties in comparing *hydrodynamic* and *geometric* radii as discussed in the main text, the radius is only overestimated by *ca.* 10% compared to the effective radius obtained from Electron Tomography. However, to obtain volume information from this radius, a spherical approximation is necessitated due to the lack of shape information obtainable from DLS data, and this corresponds to an overestimation in volume of *ca.* 30%. Furthermore, the overestimation in particle size distribution width is striking; even for monodisperse samples of polystyrene beads, DLS returns a wide distribution of sizes.[4] This is reflected in the results presented in Figure 2 of the main text. It is well documented in the literature and by the manufacturer, Malvern, that conversion of the intensity distribution to a volume or number distribution compounds any measurement error already present, but they also recommend the data obtained from the number distribution for comparison with other 'number' based techniques such as the TEM used in this work.[5] Surprisingly, the weighted number mean obtained from DLS measurements is dramatically lower than that obtained from Electron Tomography, corresponding to an underestimation in radius of *ca.* 18%, and an underestimation in volume of *ca.* 45%. This further highlights the inaccuracies in the use of DLS as a particle-sizing technique.

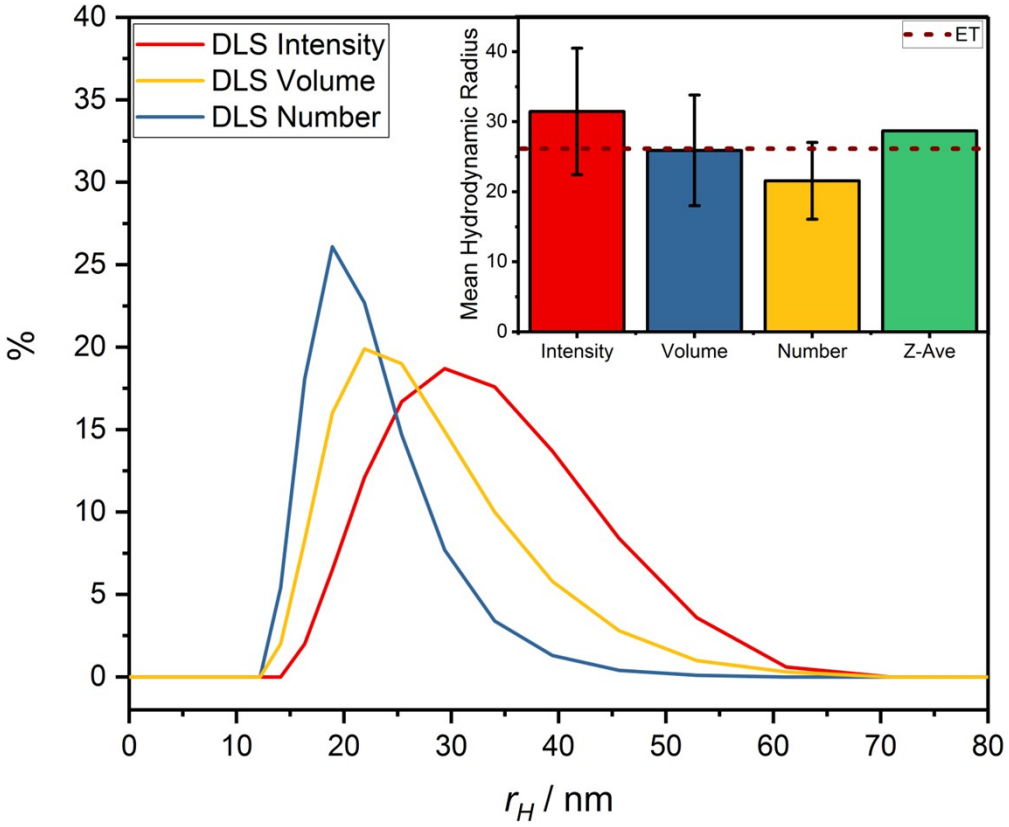

Figure S8. Normalised DLS intensity, volume and number distributions with hydrodynamic radius. Inlay depicts corresponding mean hydrodynamic radii and associated standard deviation, as well as the *z*-average radius obtained from the intensity distribution.

References

[1] M. D. Hanwell, U. Ayachit, D. A. Muller, R. Hovden, "The Tomviz Project," can be found under https://tomviz.org/, **2018**.

[2] R. C. Gonzalez, R. E. Woods, *Digital Image Processing (3rd Edition)*, Prentice-Hall, Inc., Upper Saddle River, NJ, USA, **2006**.

[3] Malvern Panalytical, "Dynamic Light Scattering," can be found under https://www.malvernpanalytical.com/en/learn/knowledge-center/whitepapers/WP111214DLSTermsDefined, **2018**.

[4] V. Filipe, A. Hawe, W. Jiskoot, *Pharm. Res.* **2010**, *27*, 796–810.

[5] Malvern Panalytical, "Intensity-Volume-Number, Which Size is Correct?," can be found under https://www.malvernpanalytical.com/en/learn/knowledge-center/technical-notes/TN101104IntensityVolumeNumber.html, **2018**.